arXiv:1611.00805v1 [physics.atom-ph] 30 Sep 2016

High harmonic generation from bulk diamond driven by intense femtosecond laser pulse

Tzveta Apostolova, Boyan Obreshkov

Institute for Nuclear Research and Nuclear Energy,

Bulgarian Academy of Sciences, Tsarigradsko chausseé 72, Sofia 1784, Bulgaria

Abstract

We investigate the high-harmonic generation (HHG) from bulk diamond induced by intense 15 fs laser pulse and photon energy 1.55 eV. For laser intensity in the range $I \in [1, 50]$ TW/cm^2, we find that HHG spectra from diamond exhibits two plateaus with high harmonics extending beyond the 50th order. Consistently with experimental observations, we find that the cutoff energy of the two plateaus scales linearly with the field strength. The first plateau arises due to recombination of electron-hole pairs near the Brillouin zone centre. The appearance of weak second plateau region for high field strength with $F \sim 1$ V/$\mathring{A}$ results in emission of highly energetic XUV photons.

PACS numbers:

I. INTRODUCTION

Nowadays EUV, XUV and soft x-ray radiation is obtained at FEL accelerator [1] and Synchrotron Radiation (SR) [2] installations that are very expensive and are still unavailable for commercial use. In the field of laser - atom interaction physics has been demonstrated that high intensity laser pulses in the UV and IR spectrum generate high order harmonics of the driving fundamental frequency [3–5]. Sources based on high harmonic generation (HHG) have the advantage of possessing spatial and temporal coherence, high directionality and polarization and the disadvantage of being far less energetic than those produced in the huge facilities. Nevertheless they can be used to obtain coherent radiation of sub-femtosecond to attosecond duration in a broad wavelength range (UV to X-ray) [6] with many possible applications such as attosecond electron dynamics , molecular tomography and protein crystallography [7, 8], etc. Theoretically the generation of ultrashort pulses of harmonics is described semi-classically by a three step model[9, 10], that is, ionization , acceleration and recombination of the emitted electron with the parent ion.

Experimental studies of HHG in solids have been reported recently, e.g. [11, 17]. In solid crystals the interplay between generation of carriers via multiphoton excitation over the bandgap at high intensities leading to catastrophic breakdown of the material and HHG is carefully explored to find regimes in which only HHG takes place avoiding material collapse [11]. In this study long wavelength laser radiation is used to suppress multiphoton ionization.

Usually the atomic HHG spectrum consists of sub-bandgap harmonics, a plateau region and a high energy cutoff region where the harmonic intensity drops off abruptly. The atomic HHG model predicts that the cutoff of the harmonic spectrum is proportional to the laser intensity. The experiments in solids show that apart from the ubiquitous sub-bandgap harmonics a second plateau is observed [12] for high laser intensities and cutoff which scales linearly with the laser field. Moreover gas-phase harmonics display fine structure for certain harmonic orders [13]. This fine structure reveals non-perturbative effects in the electron dynamics, which has not been discussed in the literature for solid-phase HHG.

There are several theoretical models [14], [15] to rationalize HHG in crystalline solids. A comparison of the HHG generation from atoms and solids was made [16]. Very recently a combined experimental and theoretical study of HHG spectra from rare-gas solids [17] exposed characteristic features of HHG in solids: abrupt appearance of a second plateau

as the driving laser intensity increases over a narrow intensity range consisting of a few harmonics; complicated dependence of the cutoff of both plateaus on the laser field, i.e. following neither linear (gas) nor the square-root scaling (solids).

In the present work we explore the feasibility for femto and attosecond pulse generation from diamond subjected to intense 15 fs laser pulse with mid-infrared wavelength. The paper is organized as follows: In Section II the theoretical framework of photoexcitation and generation of high harmonics is presented. Section III presents numerical results on the HHG spectra and analysis of non-adiabatic effects associated with HHG. Section IV inlcudes our main conclusions.

II. FORMALISM

In velocity-gauge, the TDSE in single-active electron approximations is given by

$$i\frac{d}{dt}|\psi_{v\mathbf{k}}(t)\rangle = (H_0 + H_{\rm int}(t))|\psi_{v\mathbf{k}}(t)\rangle \tag{1}$$

where $v\mathbf{k}$ labels the initially occupied valence band states of definite crystal momentum $\mathbf{k}$, H_0 is the Hamiltonian of the undistorted lattice

$$H_0 = \frac{1}{2}\mathbf{p}^2 + V(\mathbf{r}), \tag{2}$$

and

$$H_{\rm int}(t) = \mathbf{A}(t)\cdot\mathbf{p} \tag{3}$$

is the interaction Hamiltonian between the laser field and the electron, $\mathbf{p}$ is the momentum operator and $V(\mathbf{r})$ is the periodic ion-lattice potential. The vector potential is parametrized by

$$\mathbf{A}(t) = \mathbf{e}e^{-\log(4)t^2/\tau_L^2}\sin(\omega_L t) \tag{4}$$

where $\mathbf{e} = (1,1,1)/\sqrt{3}$ is a unit vector in the direction of the electric field, ω_L is the laser frequency corresponding to photon energy $\hbar\omega_L = 1.55$ eV and $\tau_L = 15$ fs is the pulse length.

The optically-induced electron current in direction of the laser electric field is given by a Brillouin zone integral

$$J(t) = \int_{\rm BZ}\frac{d^3\mathbf{k}}{4\pi^3}J(\mathbf{k},t) \tag{5}$$

where

$$J(\mathbf{k},t) = \sum_v \langle \psi_{v\mathbf{k}}(t)|\mathbf{e}\cdot\mathbf{p}|\psi_{v\mathbf{k}}(t)\rangle, \tag{6}$$

the diamagnetic gauge current contribution can be neglected, because it does not contribute to generation of high harmonics. The HHG spectrum can be presented as a coherent sum

$$I(\omega) = \left| \int_{\mathrm{BZ}} \frac{d^3\mathbf{k}}{4\pi^3} J_{\mathbf{k},\omega} \right| \tag{7}$$

over contributions from recombination of electron-hole pairs with wave-vector $\mathbf{k}$

$$J_{\mathbf{k},\omega} = \int dt e^{i\omega t} J(\mathbf{k},t). \tag{8}$$

The valence electron states are propagated in time for small equidistant steps of $\delta = 0.7$ attoseconds by applying the Cayley transformation

$$|\psi_v(t+\delta)\rangle \approx \left(I - i\frac{\delta}{2}H(t)\right)^{-1}\left(I + i\frac{\delta}{2}H(t)\right)|\psi_v(t)\rangle \tag{9}$$

where I is the unit matrix.

III. NUMERICAL RESULTS AND DISCUSSION

Fig.1(a-c) shows HHG spectra for three laser intensities $I = 2, 10$ and 30 TW/cm^2. For the low intensity shown in Fig.1(a), the HHG is characterized by odd harmonic structure due to the inversion symmetry of the diamond lattice and consists of the 1st and 3rd sub-bandgap harmonics and the 5th harmonic. Since the direct band gap at the Γ-point is nearly 7 eV, the lowest excitation of valence electrons across this gap occurs via 5 photon absorption. At this lower intensity, the HHG ends abruptly at the position of 5th harmonic, such that the high-energy cutoff is determined by the direct gap. Careful look shows that the position of 5th harmonic is red-shifted, reflecting a time delay in the emission of that harmonic relative to the pulse peak. For the increased intensity shown in Fig.1(b), the spectrum extends to higher harmonic orders, a single plateau appears with cut-off at the position of 9th harmonic. Noticeably individual harmonics exhibit fine structure, similarly to the results reported for the gas phase [13]; the inset shows the line shape of the 5th harmonic peak, it displays additional multipeak structure near the line center. Within a classical re-collision model for the gas phase, this additional structure of harmonic peaks is explained in terms of interferences between those parts of the wavepacket that are reflected by the ionic

core and the ones that are still incoming [18]. For the highest intensity 30 TW/cm^2 shown in Fig.1(c), a second plateau suddenly emerges with cutoff positioned at the 50th harmonic. The appearance of second plateau with harmonic orders extending beyond the atomic limit of the corresponding gas-phase harmonics indicates strong dependence of HHG on the band structure of diamond. Similar results are found in HHG spectra from rare-gas solids [17].

Fig.2(a-b) shows the field-dependence of the photon-energy cutoff for the first and second plateau, respectively. In contrast to the cutoff law observed for gas-phase harmonics, cutoff harmonics generated from diamond bulk display almost linear scaling with the field strength F. This linear scaling law is consistent with experimental observations in ZnO [11]. The high-energy cutoff of the second plateau is distinguishable for strong fields with $F \sim 0.4V/\mathring{A}$ corresponding to laser intensity $I > 10$ TW/cm^2. The slope of this linear dependence implies that the cutoff energy increases by 2 harmonic orders when the field strength is increased by $0.5V/nm$. In contrast, the slope of the photon-energy cutoff of the first plateau is flatter by a factor of 3.

In Fig.3 we plot the field dependence of the spectral intensity of individual harmonics S_n from the first plateau. The laser intensity dependence can be divided into 3 regimes. I. Perturbative regime: The 3rd and the 5th harmonic are distinguishable and scaling law $S_n \sim F^n$ is exhibited. II. Intermediate regime (with $F \sim 1$ V/nm): The HHG spectrum extends to higher orders as the field strength increases. The intensity of different harmonic orders show the same power law $S_n \sim F^6$ regardless on the harmonic order. III. High field strength with $F \geq 5$ V/nm: the intensity of individual harmonics become indistinguishable.

To rationalize the above trends, Fig.4(a-c) presents the time evolution of the current density distribution for three different laser intensities I =2,10 and 30 TW/cm^2. In the perutbrative regime shown in Fig.4(a), the current density follows quasi-adiabatically the laser vector potential, i.e.

$$J(\mathbf{k},t) \approx \sum_v \mathbf{e}\cdot\nabla_{\mathbf{k}}\varepsilon_v(\mathbf{k})\Big|_{\mathbf{k}=\mathbf{k}(t)} \tag{10}$$

where $\mathbf{k}(t) = \mathbf{k} + \mathbf{A}(t)$ is the shifted crystal momentum and $\varepsilon_v(\mathbf{k})$ are dispersion curves for valence electrons. For the intermediate regime in Fig.4(b), the time evolution of photoexcited carriers with momenta near the BZ edges remains adiabatic due to the wide band gaps of diamond, however states near the BZ center do not have enough time to fully equilibrate against the laser vector potential $A(t)$, such that the current density is strongly distorted

after the peak of the pulse. This distortion expresses the non-adiabatic effects of electron-hole pair excitation as we discuss below. The nonlinear polarization current undergoes rapid changes on a sub-femtosecond (attosecond) time scale tracing out a burst of emitted high harmonics after the peak of the pulse. For high field strength with intensity $I = 30$ TW/cm^2, the prompt excitation of electron-hole pairs becomes highly likely as shown in Fig.4(c) and the non-adiabatic distortion of the current density extends over higher momentum states in the BZ.

The Fourier transform of the even part of the current density $I(\mathbf{k}, \omega) = |J_{\mathbf{k}\omega} + J_{-\mathbf{k},\omega}|$ along the Γ-L line is shown in Fig.5(a-c) . The odd harmonic structure of HHG is due to the destructive interference of even order harmonics. For the lowest intensity in Fig.5(a), sub-bandgap harmonics extend from the BZ center towards the edges; the recombination of electron-hole pairs near the BZ center gives rise to intense emission of 5th harmonic, while the 7th order is highly virtual and suppressed. For higher laser intensity $I = 10$ TW/cm^2 shown in Fig.5(b), the HHG spectrum is characterized by the plateau region above the bandgap with cutoff at the position of the 9th harmonic. The numerical results reveal that the plateau and the the high-energy cutoff converge when at least 8 conduction bands are included, and therefore the simple linear dependence of the cutoff law on the field strength has non-trivial dependence on the substrate band structure and is characterized by strong coupling involving multiple single-particle states. For the highest intensity shown in Fig.5(c), the spectrum extends to high harmonic orders. The two plateau regions can be distinguished, the first one extends to 15th order, decreases gradually in spectral intensity with the increase of the harmonic order and crosses over into the second plateau with harmonics extending above the 40th order.

To non-adiabatic electron dynamics associated with HHG in the intermediate regime with laser intensity 10 TW/cm^2 is shown in Fig. 6(a-c). Fig. 6(a) shows the temporal profile of the nonlinear current corresponding to 5-photon transition from the light-hole into the lowest conduction band ($n_c = 1$). The current waveform follows adiabatically the laser vector potential during the first part of the pulse and is distorted 2fs prior to the peak of the pulse; the subsequent rapid sub-cylce oscillations represent the build up of coherent superposition of populations in the valence and the conduction band; steady-state dipole oscillations remain after the end of the pulse. Quite similarly, the laser-induced hybridization of the light-hole valence with a higher-lying conduction band ($n_c = 2$) creates rapid dipole

oscillations on an attosecond time scale, cf. Fig. 6(b). The enhanced steady-state non-adiabatic current gives rise to emission of intense 7th harmonic at the end of the pulse. Fig. 6(c) shows the nonlinear current corresponding to transitions into and out of the $n_c = 5$ conduction band, noticeablythe peak of the current is delayed by 5 fs after the peak of the pulse, the time profile shows that the 9th cutoff harmonic is highly virtual and exists only during the second half of the pulse. Similar results are found in the strong-field regime, the second plateau is due to interband transitions into higher-lying conduction bands,

IV. CONCLUSION

We presented calculation of HHG spectrum from bulk diamond induced by an intense femtosecond laser pulse. Our result describes the intense HHG extending from the perturbative to highly non-perturbative incident laser intensity regimes. The non-perutrbative regime of HHG occurs for laser intensity $I \geq 1TW/cm^2$. We find that the HHG spectra from diamond exhibit two plateaus, the second plateau extending beyond the limit of the corresponding gas-phase harmonics emitted for the same laser intensity. We find that HHG and cutoff law are sensitive to details of the substrate band structure involving strong interband couplings between multiple single-particle states. We have shown that the first plateau is due to transitions between the valence band and the few lowest conduction bands, whereas the secondary plateau involves contributions from higher-lying conduction bands. The numerical results make evident the feasibility of diamond for sub-femtosecond pulse generation.

[1] M. Abd-Elmeguid et al., Tesla Technical Design Report, The X-ray Free Electron Laser (DESY, Hamburg, 2001)

[2] H. Winick Ed., Synchrotron Radiation Sources, World Scientific Pub. Co. Inc., World Scientific Series on Synchrotron Radiation Techniques(1995).

[3] A. McPherson, G. Gibson, H. Jara, U. Johann, T. S. Luk, I. A. McIntyre, K. Boyer, and C. K. Rhodes, J. Opt. Soc. of Am. B **4**, 595-601 (1987).

[4] M. Ferray, A. L'Huillier, X. F. Li, L. A. Lompre, G. Mainfray and C. Manus, J. Phys. B: At. Mol. Opt. Phys. **21** L31, (1988).

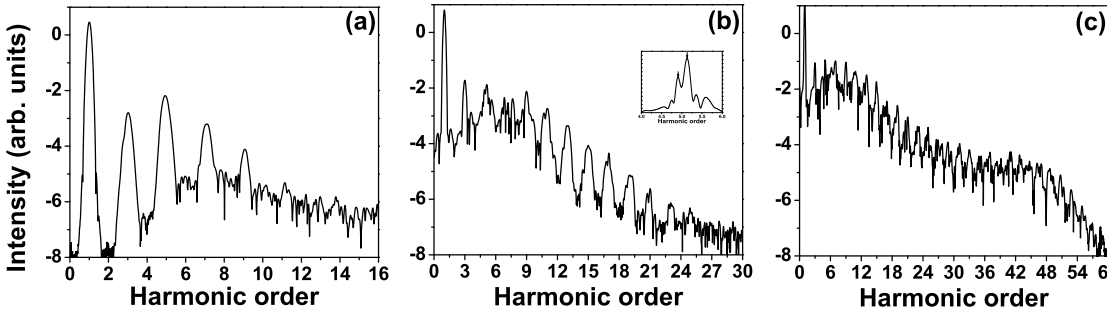

FIG. 1: HHG spectra from bulk diamond for 15 fs laser pulse with photon energy 1.55 eV . The laser intensity in Fig.(a), Fig.(b) and Fig.(c) is 2,10 and 30 TW/cm^2, respectively.

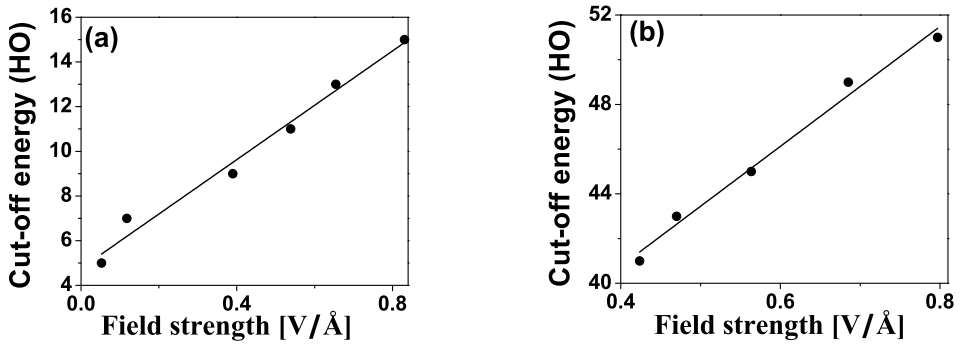

FIG. 2: High-energy cutoff as a function of the driving laser field for the first plateau in Fig.(a) and the second plateau in Fig.(b)

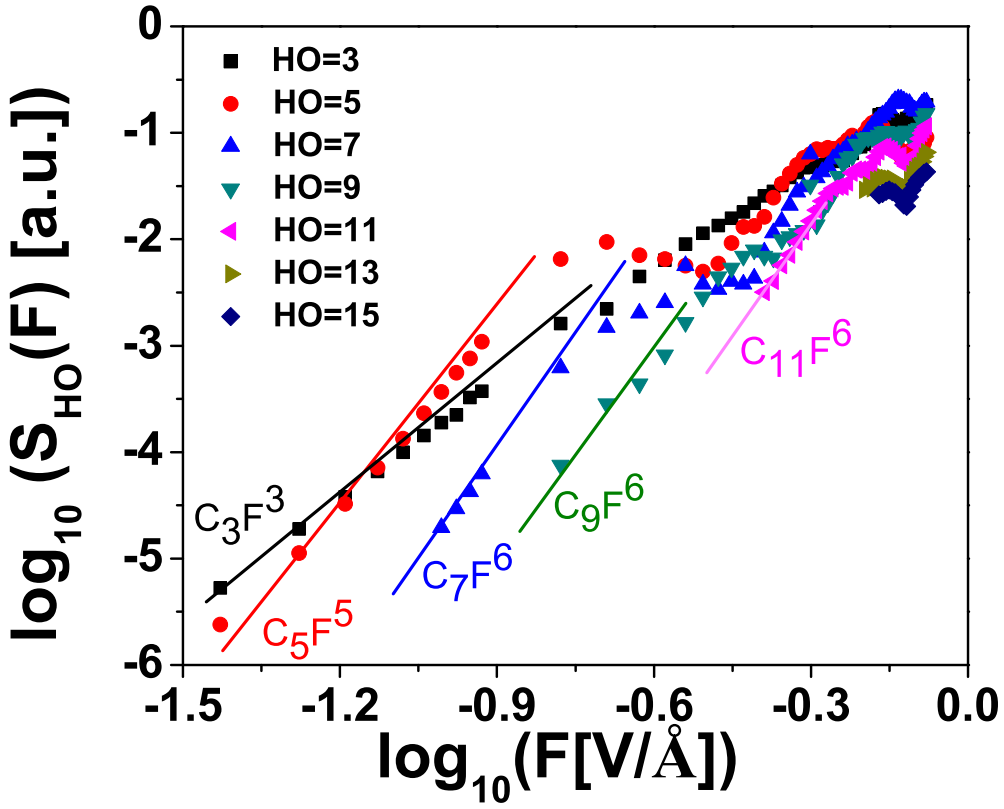

FIG. 3: Dependence of the spectral intensity of individual harmonics on the electric field strength for 15fs laser pulse with photon energy 1.55 eV interacting with bulk diamond.

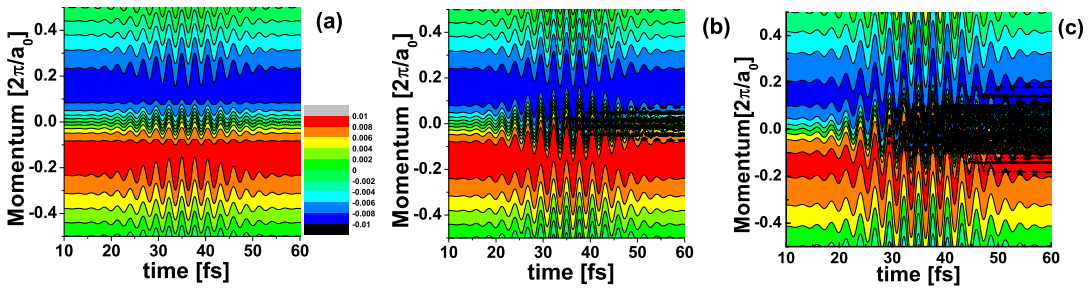

FIG. 4: Optically induced current density in diamond bulk along the Γ-L line in the Brillouin zone. The laser intensity is $I = 2TW/cm^2$ in Fig.(a), $I = 10TW/cm^2$ in Fig.(b) and $I = 30TW/cm^2$ in Fig.(c).

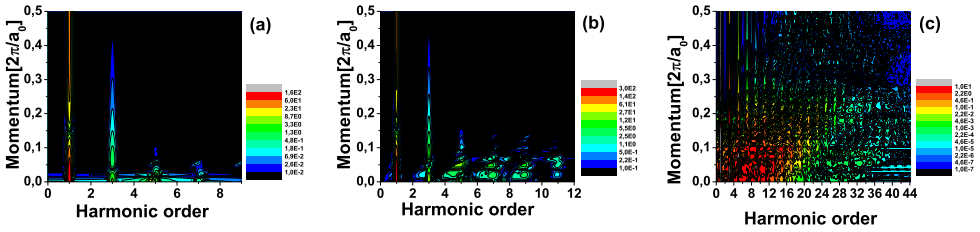

FIG. 5: Fourier transform of the current density in diamond bulk along the Γ-L line in the Brillouin zone. The laser intensity is $I = 2TW/cm^2$ in Fig.(a), $I = 10TW/cm^2$ in Fig.(b) and $I = 30TW/cm^2$ in Fig.(c).

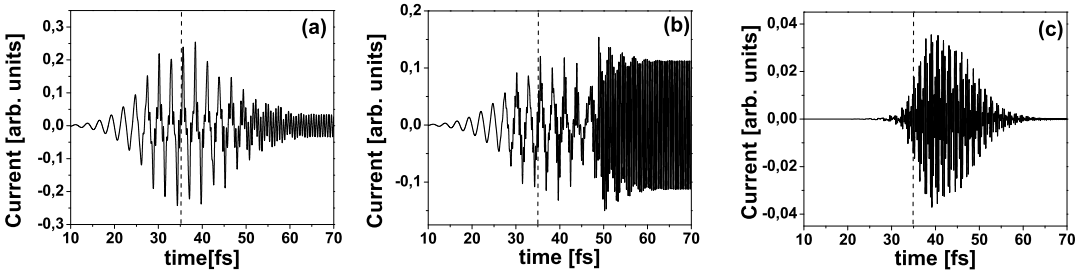

FIG. 6: Time evolution of the optically-induced polarization current corresponding to recombination of electrons with the light-hole band close to the BZ center. Fig. (a) 5-photon transition into the lowest conduction band ($n_c = 1$), Fig.(b) 7-photon transition into the first excited conduction band ($n_c = 2$). Fig.(c) presents the temporal profile of the current associated with the emission of 9th cutoff harmonic. In Fig. (a-c) the laser intensity is $I = 10$ TW/cm^2 and the crystal momentum

[5] K. C. Kulander, K. J. Schafer, J. L. Krause, Super-Intense Laser-Atom Physics. Ed. B. Piraux, A. L'Huillier, and K. Rzazewski. D. Reidel Publishing Company, Dordrecht-Holland. NATO Advanced Study Institutes Series. B **316**, 95 (1993).

[6] P. B. Corkum and F. Krausz, Attosecond Science, Nat. Phys., 3, 381, (2007)

[7] Martin Schultze, Krupa Ramasesha, C.D. Pemmaraju, S.A. Sato, D. Whitmore, A. Gandman, James S. Prell, L. J. Borja, D. Prendergast, K. Yabana, Daniel M. Neumark, Stephen R. Leone, Science 12 Dec 2014: Vol. 346, Issue 6215, pp. 1348-1352, DOI: 10.1126/science.1260311

[8] N. H. Chapmann, P. Fromme, A. Barty et al, Nature **470**, 73 (2011).

[9] K. J. Schafer, B. Yang, L. F. DiMauro, and K. C. Kulander, Phys. Rev. Lett. **70**, 1599 (1993).

[10] P. B. Corkum, Phys. Rev. Lett. **71**, 1994.

[11] S. Ghimire et al, Nature Physics **3**, 381 (2011).

[12] M. Wu, S. Ghimire, D. A. Reis, K. J. Schafer, and M. B. Gaarde, Phys. Rev. A **91**, 043839, (2015).

[13] X. Chu, S-I. Chu, C. Laughlin, Phys. Rev. A **64**, 013406 (2001).

[14] G. Vampa, C. R. McDonald, G. Orlando, D. D. Klug, P. B. Corkum, and T. Brabec, Phys. Rev. Lett. **113**, 073901 (2014).

[15] T. Higuchi, M. I. Stockman, and P. Hommelhoff, Phys. Rev. Lett. **113**, 213901, (2014).

[16] G. Vampa, T. J. Hammond, N. Thiré, B. E. Schmidt, F. Légaré, C. R. McDonald, T. Brabec, P. B. Corkum, Nature **522**, 462 (2015).

[17] G. Ndabashimiye, S. Ghimire, M. Wu, D. A. Browne, K. J. Schafer, M. B. Gaarde and D. A. Reis, Nature **522**, 462 (2016).

[18] M. Protopapas, C. H. Keitel and P. L. Knight, Rep. Prog. Phys. **60** 389, (1997).

[19] S. Lagomarsino, S. Sciortino, B. Obreshkov, T. Apostolova, C. Corsi, M. Bellini, E. Berdermann, and C. J. Schmidt, Phys. Rev. B **93**, 085128, (2016).

[20] G. Vampa, C. R. McDonald, G. Orlando, P. B. Corkum, and T. Brabec, Phys. Rev. B **91**, 064302 (2015).